

# Persistent Replicative Stress Alters Polycomb Phenotypes and Tissue Homeostasis in *Drosophila melanogaster*

Severine Landais,<sup>1</sup> Cecilia D'Alterio,<sup>1,2</sup> and D. Leanne Jones<sup>1,2,\*</sup>

<sup>1</sup>Laboratory of Genetics, The Salk Institute for Biological Studies, La Jolla, CA 92037, USA

<sup>2</sup>Department of Molecular, Cell, and Developmental Biology, University of California, Los Angeles, Los Angeles, CA 90095, USA

\*Correspondence: [leannejones@ucla.edu](mailto:leannejones@ucla.edu)

<http://dx.doi.org/10.1016/j.celrep.2014.03.042>

This is an open access article under the CC BY-NC-ND license (<http://creativecommons.org/licenses/by-nc-nd/3.0/>).

## SUMMARY

Polycomb group (PcG) proteins establish and maintain genetic programs that regulate cell-fate decisions. *Drosophila multi sex combs (mxc)* was categorized as a PcG gene based on a classical Polycomb phenotype and genetic interactions; however, a mechanistic connection between Polycomb and Mxc has not been elucidated. Hypomorphic alleles of *mxc* are characterized by male and female sterility and ectopic sex combs. Mxc is an important regulator of histone synthesis, and we find that increased levels of the core histone H3 in *mxc* mutants result in replicative stress and a persistent DNA damage response (DDR). Germline loss, ectopic sex combs and the DDR are suppressed by reducing H3 in *mxc* mutants. Conversely, *mxc* phenotypes are enhanced when the DDR is abrogated. Importantly, replicative stress induced by hydroxyurea treatment recapitulated *mxc* germline phenotypes. These data reveal how persistent replicative stress affects gene expression, tissue homeostasis, and maintenance of cellular identity in vivo.

## INTRODUCTION

Proper development and tissue homeostasis require stabilization of cell identity as well as plasticity of gene expression. The Polycomb group (PcG) proteins are chromatin modifiers that act as transcriptional repressors, which were first described in *Drosophila* more than 30 years ago. Originally, they were characterized as regulators of homeotic gene expression, such as the *Hox* genes, that pattern the anterior-posterior body plan during development (Lewis, 1978); however, since that time, PcG proteins have been demonstrated to be conserved across species and play important roles in regulating stem cell behavior and cancer progression (Sauvageau and Sauvageau, 2010).

Two core complexes composed of canonical PcG proteins, Polycomb repressive complexes 1 and 2 (PRC1 and PRC2), have been described; however, the composition of PRCs is var-

iable and context dependent. One role for PRC2 is methylation of histone H3 on lysine 27 to generate H3K27me3, a modification thought necessary to recruit PRC1, which can then catalyze histone H2A monoubiquitylation on lysine 119 (K118 in *Drosophila*) to strengthen gene repression (Schwartz and Pirrotta, 2007). Some proteins have been classified as PcG proteins based on association with PRC 1 or 2 (Sparmann and van Lohuizen, 2006), whereas other genes, such as *Drosophila multi sex combs (mxc)*, exhibit robust genetic interactions with PcG genes but have not been found associated with either PcG complex (Saget et al., 1998; Santamaría and Randsholt, 1995).

Hypomorphic alleles of *mxc* are characterized by hematopoietic defects, male and female sterility, and a classical *Drosophila* Polycomb phenotype consisting of ectopic sex combs (Docquier et al., 1996; Santamaría and Randsholt, 1995). Recently, *mxc* was found to localize to the histone locus body (HLB) and play a key role in histone synthesis (White et al., 2011). Consequently, Mxc was proposed to be the *Drosophila* equivalent of mammalian NPAT (nuclear protein of the ataxia telangiectasia-mutated gene) (White et al., 2011). Although NPAT has been shown to be necessary for histone synthesis and cell-cycle progression in human embryonic stem cells (Becker et al., 2010; Ghule et al., 2008), no links between defects in histone synthesis and maintenance of cell fates have been demonstrated previously. Our characterization of *mxc* phenotypes has revealed that persistent replicative stress and an ongoing DNA damage response can lead to alterations in cellular identities and a loss of tissue homeostasis, resembling disruption of Polycomb function.

## RESULTS

### Mutations in *mxc* Disrupt Germline Homeostasis

Two populations of adult stem cells reside at the tip of the *Drosophila* testis: the germline stem cells (GSCs) and somatic cyst stem cells (CySCs). GSCs and CySCs are in direct contact with a cluster of somatic cells, known as the hub, that serve as a critical component of the stem cell niche (Kiger et al., 2001; Leatherman and Dinardo, 2010; Tulina and Matunis, 2001) (Figure 1A). GSCs divide asymmetrically to generate another GSC and a gonialblast, which is displaced away from the hub and initiates differentiation by undergoing four rounds of mitotic, transit

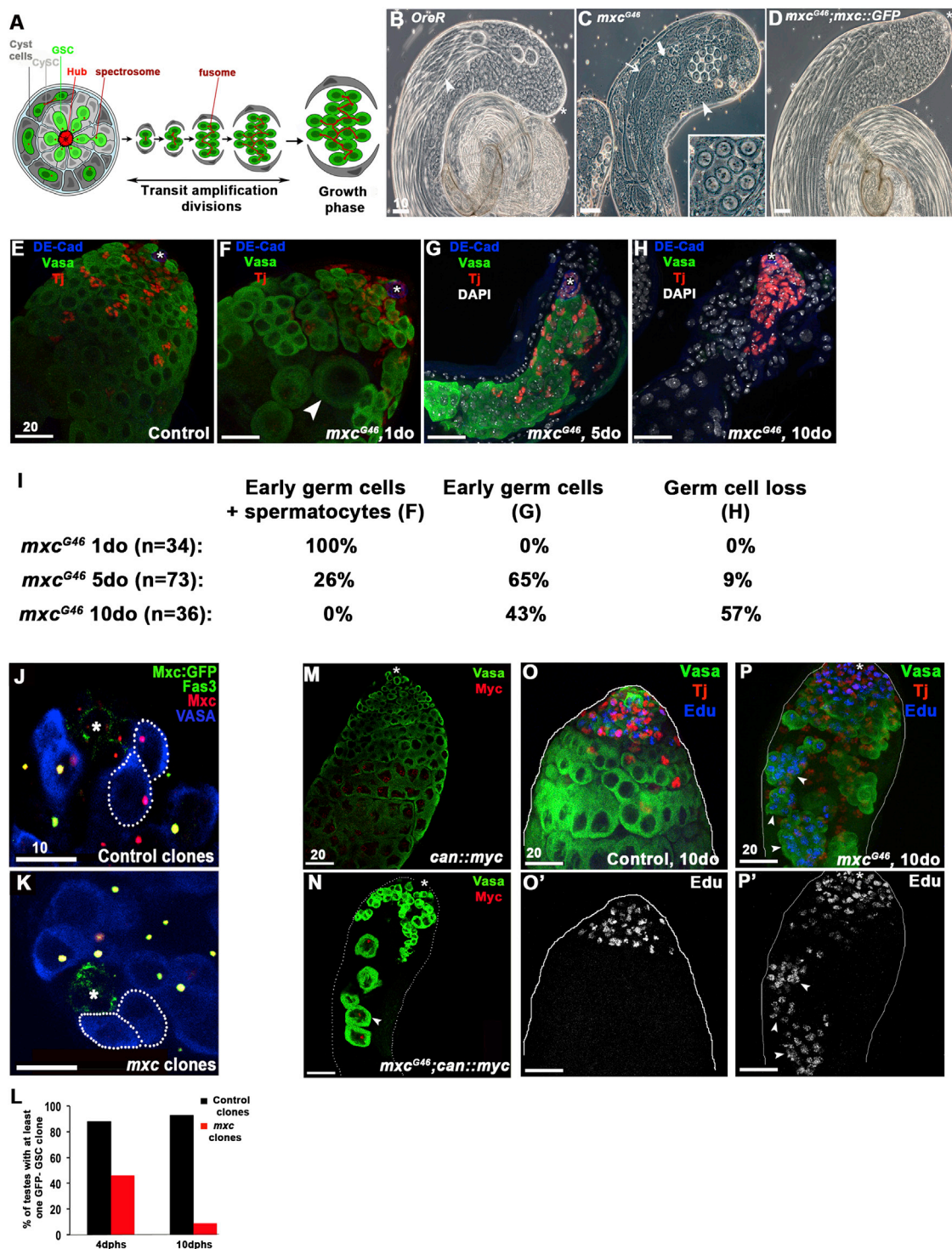


**Figure 1. Mutations in *mx<sup>G46</sup>* Result in Germ Cell Loss over Time**

(A) Schematic of *Drosophila* spermatogenesis. GSC, germline stem cell; CySC, cyst stem cell.

(B) Phase contrast image of a normal testis showing the spatial gradient of germ cell development. GSCs and spermatogonia are located at the tip (asterisk), followed by spermatocytes in growth phase, meiotic germ cells, haploid spermatids, and mature sperm, visible in the lumen of the testis (arrowhead).

(C) Testes mutant for *mx<sup>G46</sup>* show loss of germ cells but differentiated cell types are present (spermatid cyst at onion stage, arrowhead; spermatocytes, thick arrow; elongating spermatids, thin arrow). Cysts of <16 germ cells are often observed (inset).

(D) The *mx<sup>G46</sup>* testis phenotype is completely rescued by a *mx<sup>G46</sup>::GFP* transgene.

(legend continued on next page)

amplification (TA) divisions with incomplete cytokinesis, to generate a cyst of 16 interconnected spermatogonia. After pre-meiotic S phase, spermatogonia increase in volume approximately 25 times, differentiate into spermatocytes, and undergo meiosis to generate mature, haploid sperm (Figures 1A and 1B) (Fuller, 1993).

Although the effects of the *mx*c mutation are not specific to germ cells, the weakest, viable allele of *mx*c, *mx*c<sup>G46</sup>, distinguishes itself by having a dramatic germline phenotype (Figures 1C and S1A). An *mx*c::GFP transgene completely rescued lethality of animals carrying the strongest *mx*c alleles, as well as the germline defects present in *mx*c<sup>G46</sup> mutant males (Figure 1D). Consistent with previous results, Mxc localized to discrete subnuclear foci in all cells throughout the testis, corresponding to the histone locus body (HLB) (White et al., 2011) (Figures S1B and S1C). Tissue homeostasis is severely compromised in testes from *mx*c<sup>G46</sup> mutants, with loss of germ cells and disruption of the normal spatiotemporal gradient of germ cell development and differentiation (Figures 1B and 1C). A detailed characterization of the effect of *mx*c<sup>G46</sup> mutations on the adult male germline revealed three distinct phenotypes: (1) testes containing disorganized spermatogonia and larger germ cells harboring characteristics of mature spermatocytes (Figure 1F), (2) testes containing only spermatogonia (Figure 1G), and (3) complete loss of the germline, with clusters of somatic cyst cells adjacent to the hub (Figure 1H). Over time, the percentage of testes with complete loss of the germline increased significantly (Figure 1I).

Somatic cyst cells strongly influence the behavior of GSCs and spermatogonial differentiation; therefore, *mx*c function could be required in germ cells, somatic cells, or both, resulting in the observed germline defects in *mx*c mutant males. In order to determine whether *mx*c acts cell autonomously to regulate GSC maintenance, FRT-mediated clonal analysis was used to generate germ cells that were homozygous mutant for the null *mx*c<sup>G48</sup> allele (Figure S1A) (see Experimental Procedures for details) (Xu and Rubin, 1993). In comparison to *mx*c<sup>+</sup> GSCs, significantly fewer *mx*c<sup>G48</sup> mutant GSCs were maintained over time (Figures 1J–1L), suggesting that *mx*c acts autonomously in the germline to regulate maintenance of GSCs. This is consistent with the loss of GSCs in newly eclosed (hatched) 1-day-old (1 d.o.) *mx*c mutant males (control [*w*–]: 9.9 ± 2.5 SD [*n* = 16]; *mx*c<sup>G46</sup>/Y: 6.2 ± 2.0 [*n* = 18]; *mx*c<sup>G43</sup>/Y: 4.1 ± 3.3 [*n* = 18]).

Importantly, the loss of germ cells in *mx*c mutant males is not due to an inability to undergo cell division, because *mx*c mutant spermatogonial cysts were observed frequently (Figure S1D). Furthermore, in newly eclosed *mx*c<sup>G46</sup> males, large germ cells in groups of <16 are observed that express markers of differentiation, such as the spermatocyte marker *cannonball* (*can*) (Figures 1C, 1F, 1M, and 1N). Thus, early germ cells appear to undergo mitosis but initiate a terminal differentiation program before completion of the four TA divisions. Furthermore, germ cells in testes from *mx*c<sup>G46</sup> males incorporate EdU, a thymidine analog, indicating that cells continue to proliferate and progress through S phase. However, EdU<sup>+</sup> germ cells begin to accumulate throughout the testis in 5 and 10 d.o. *mx*c<sup>G46</sup> males, suggesting that these germ cells stall in or undergo a protracted S phase (compare Figures 1O and 1O' to 1P and 1P'). The increase in cells in S phase is coupled with a noticeable absence of cells in mitosis, as revealed by a decrease in cells staining positive for the mitosis marker phosphorylated histone H3 (Figure S1F). Therefore, our data suggest that the eventual loss of germ cells in *mx*c mutant testes results from a failure to maintain GSCs, premature initiation of terminal differentiation, and accumulation of spermatogonia in S phase, followed by germ cell loss.

### Mxc Regulates Maintenance and Differentiation of the Somatic Lineage in the Testis

Somatic cells play an integral role in regulating the behavior of male germ cells in the testis (Kiger et al., 2000; Leatherman and Dinardo, 2008, 2010; Matunis et al., 1997; Tran et al., 2000). Early somatic cyst cells expressing the transcription factor Traffic Jam (TJ) appeared relatively unaffected in testes from males carrying the weakest *mx*c<sup>G46</sup> allele (Figures 1E–1H). Therefore, we wanted to determine whether *mx*c also regulates somatic cell behavior, which could contribute to the loss of germ cells observed in *mx*c mutants. To reduce *mx*c expression in CySCs and early cyst cells in adults, we used the bipartite GAL4-UAS system (Brand et al., 1994) in combination with RNAi-mediated knockdown of gene expression. An *mx*cRNAi transgene was expressed under control of the *c587GAL4* driver, and flies were raised at 18°C during development to restrict RNAi transgene expression to adult stages. Upon eclosion (hatching), adult flies were shifted to 29°C to induce expression of *mx*cRNAi in somatic cells surrounding spermatogonia, and knockdown was confirmed by antibody staining (Figures 2A–2B').

(E) Control testis filled with Vasa<sup>+</sup> germ cells (green), Traffic-Jam<sup>+</sup> (Tj<sup>+</sup>) somatic cyst cells (red), and hub cells (asterisk) expressing DE-Cad<sup>+</sup> (blue).

(F) *mx*c<sup>G46</sup> testis contains large spermatocytes (arrowhead) intermingled with spermatogonia and early spermatocyte cysts.

(G) *mx*c<sup>G46</sup> testis containing spermatogonia and cyst support cells only. Note absence of spermatocytes.

(H) *mx*c<sup>G46</sup> testis completely devoid of germ cells.

(I) Table representing increasing severity of *mx*c<sup>G46</sup> testes phenotype over time (1–10 days old).

(J) Control GSC clones (Vasa<sup>+</sup>, blue, dashed lines) around the hub (Fas3<sup>+</sup>, green, asterisk), induced by FRT-mediated loss of an *mx*c::GFP rescue transgene (green in J), still express endogenous Mxc (red).

(K) GSC clones homozygous mutant for *mx*c<sup>G48</sup> do not express *mx*c::GFP nor endogenous Mxc (as shown by the loss of Mxc nuclear body).

(L) *mx*c<sup>G48</sup> mutant GSCs are lost over time, whereas control GSC clones are maintained 10 days post heat shock (dphs).

(M and N) Large *mx*c<sup>G46</sup> mutant germ cells express the spermatocyte marker *cannonball* (*can*) (Myc<sup>+</sup>, red, arrowhead).

(O and O') EdU incorporation is limited to actively dividing spermatogonia in the transit amplifying (TA) region at the tip of the testis in controls. Germ cells, green (Vasa<sup>+</sup>), cyst cells, red (Tj<sup>+</sup>), EdU, blue.

(P and P') *mx*c<sup>G46</sup> mutant testis containing spermatogonia (Vasa<sup>+</sup>, green) in S phase, indicated by EdU incorporation in germ cell cysts outside of the mitotic zone (arrowheads). Scale bars indicated in μm.



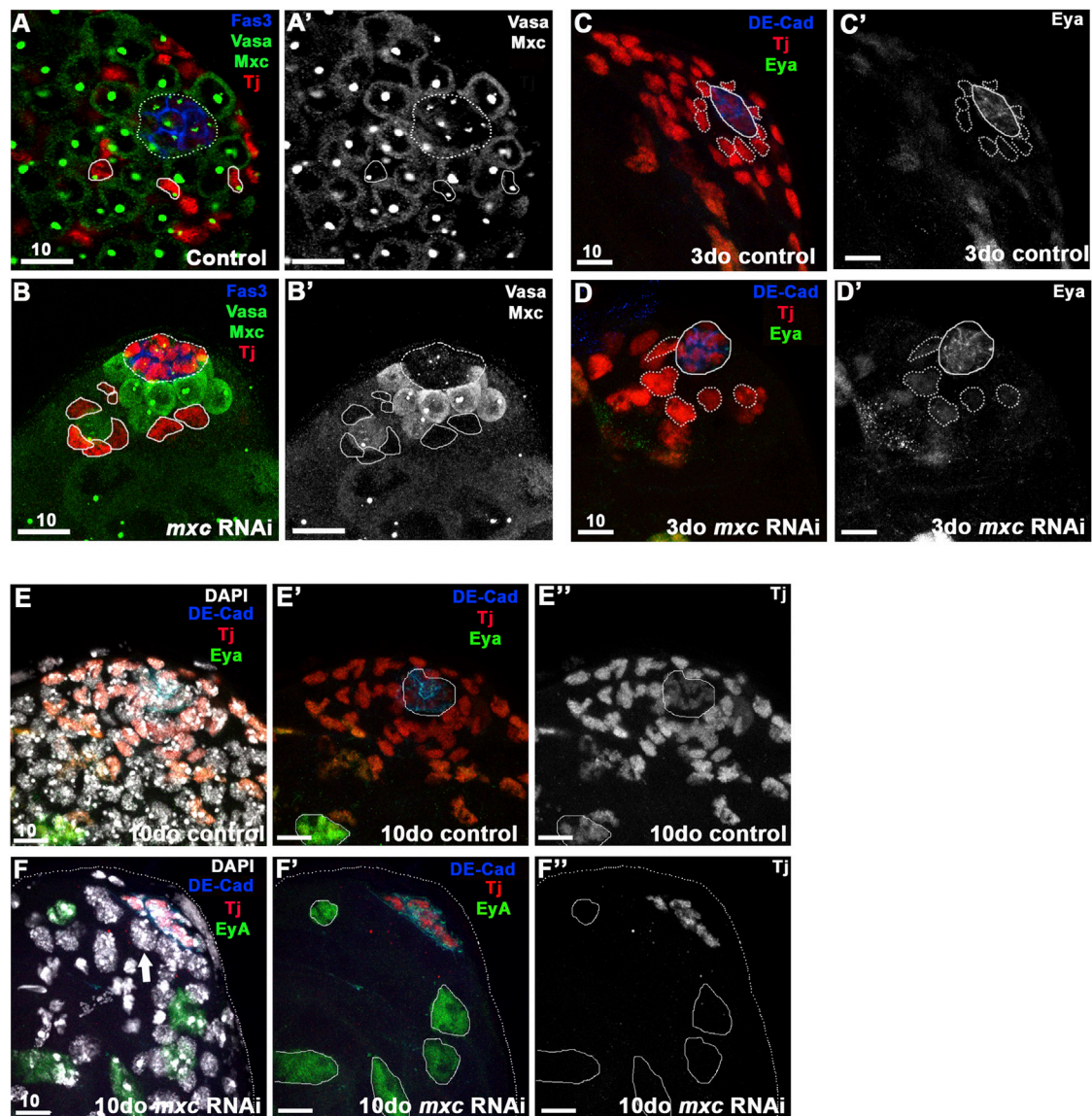


**Figure 2. Mxc Is Required Autonomously for Maintenance of Early Cyst Cells**

(A–B') RNAi-mediated knockdown of *mxc* (RNAi induced for 7 days) in early cyst cells ( $Tj^+$ , red) using the *c587GAL4* driver results in a significant reduction in cyst cells at the testis tip, including CySCs (B), when compared to controls (A). Loss of Mxc staining in cyst cells (circled, B and B' compared to A and A') confirmed efficiency of RNAi-mediated knockdown. Germ cells (Vasa, green), Mxc (HLB, green), and hub (Fas3, blue; dashed circle).

(C–D') The nuclei of  $Tj^+$  cells adjacent to the hub (CySCs, dotted line) are significantly larger 3 days after induction of *mxc*RNAi (D and D') when compared to controls (C and C') and express higher levels of the late cyst cell marker Eyes absent (Eya, green), indicating precocious differentiation. Early cyst cells ( $Tj^+$ , red), hub (DE-cad $^+$ , blue), late cyst cells (Eya $^+$ , green).

(E–F'') Ten days after induction of *mxc*RNAi, late cyst cells (Eya $^+$ / $Tj^-$ , green) replace early cyst cells ( $Tj^+$ , red) at the apical tip (F–F''). DAPI staining (white in F) reveals the presence of germ cells ( $Tj^-$ , Eya $^-$ ) at the tip of the testis, adjacent to the hub (thick arrow), similar to (B).

Scale bars indicated in  $\mu$ M.

In flies expressing *mxc*RNAi for 3 days,  $Tj^+$  cyst cells were detected at the testis tip; however, the cyst cells surrounding and in contact with the hub, typically defined as CySCs, were significantly larger when compared to cells found at that position in control testes (Figures 2B, 2D, and 2D') (Gonczy and DiNardo, 1996; Leatherman and Dinardo, 2008). After 10 days, a dramatic loss of  $Tj^+$  somatic cells was observed in flies expressing

*mxc*RNAi in early cyst cells, when compared to controls (Figures 2E–2F'). Testes also appeared depleted for early germ cells (Figures 2B and 2B'), consistent with a loss of CySCs, which play an important role in regulating GSC proliferation. Notably, cyst cells that remain at the tip of the testis after *mxc* depletion express differentiation markers, such as the transcription factor Eyes absent (Eya), which is normally absent from early cyst cells but

expressed in differentiated cyst cells that surround spermatocytes (Figures 2D' and 2F–2F"). Therefore, RNAi-mediated depletion of *mx*c in somatic cells revealed that Mxc regulates maintenance and differentiation of both germline and somatic lineages in the testis.

### ***mx*c Phenotypes Are Due to Excess Histone H3**

The histone locus body (HLB) is a protein complex responsible for the transcription and 3'-end processing of nonpolyadenylated histone mRNAs (Marzluff and Duronio, 2002). As a central component of the HLB, Mxc is involved in both transcription and processing of core histone mRNAs (Salzler et al., 2013; White et al., 2011). Quantitative PCR from flies carrying strong (*mx*c<sup>G43</sup>) and weak (*mx*c<sup>G46</sup>) *mx*c alleles across different developmental stages revealed that histone mRNA levels vary over time, and not all histones are affected similarly (Figures 3A and Figure S1A). In general, higher levels of histone H3 and lower levels of histone H1 were observed earliest in the strongest *mx*c mutant backgrounds and at later developmental stages and in *mx*c<sup>G46</sup> adults. Eventually, histone mRNA levels decline (Figure 3A), consistent with previously published results (White et al., 2011).

Remarkably, RNAi-mediated knockdown of histone H3 in early germ cells completely suppressed the testis phenotype in *mx*c<sup>G46</sup> males (Figures 3B–3E'). The efficiency of H3 RNAi expression was verified using fluorescence in situ hybridization (FISH), which showed a distinct reduction of H3 mRNA in early germ cells (Figure S2). The normal gradient of germ cell differentiation and maturation was restored, including maintenance of GSCs (Figure 3F). Moreover, *mx*c<sup>G46</sup> males with continuous germline expression of H3 RNAi appear to be as fertile as control flies and give rise to normal progeny (Figure 3G). In contrast to H3, H1 levels were decreased in *mx*c mutants, but neither overexpression of histone H1 rescued nor RNAi-mediated knockdown of H1 recapitulated *mx*c phenotypes (Figure S3). Thus, an increase in the levels of histone H3 mRNA appears to be the primary cause of germline loss in *mx*c<sup>G46</sup> mutant males.

Flies mutant for *mx*c have a classical Polycomb phenotype represented by defects in the specification of sex combs (Santamaría and Randsholt, 1995). Given the suppression of the *mx*c germline phenotype by H3 RNAi, we wanted to determine whether the Polycomb phenotype, i.e., ectopic sex combs, could also be rescued by decreasing H3 levels. Sex combs are typically located on the first tarsus (T1) of the first leg (L1); however, in *mx*c<sup>G46</sup> males, sex combs are observed on additional legs and tarsi (Figure 3H), indicative of a homeotic transformation of the second and third thoracic segments into the first. In *mx*c<sup>G46</sup> flies, sex combs were found on the second tarsus (T2) of L1 in 37% of animals examined, whereas 20% exhibited sex combs on the second leg (L2) and 7% exhibited sex combs on the third leg (L3) (Figure 3H). However, conditional expression of H3 RNAi in imaginal discs of *mx*c<sup>G46</sup> mutant flies resulted in a significant decrease in the L2 to L1 and L3 to L1 transformations (Figure 3H), suggesting that higher levels of H3 due to *mx*c mutations might compromise the activity of PRCs, resulting in Polycomb phenotypes.

### ***mx*c Mutant Cells Accumulate Foci of the DNA Damage Marker $\gamma$ H2Av**

Production of new histones is tightly linked to cell-cycle progression. Histone synthesis is initiated at the G1/S transition, and new histones are incorporated immediately behind the progressing replication fork during DNA replication. However, excess histones can lead to stalling of the replication fork and present a source of replicative stress and DNA damage (Gunjan and Verreault, 2003; Herrero and Moreno, 2011; Singh et al., 2010).

Because we observed an accumulation of cells in S phase in the *mx*c mutant background (Figures 1O and 1O'), we hypothesized that these cells would exhibit hallmarks of replicative stress due to excess H3. Consistent with initiation of a DNA damage response (DDR), foci representing a phosphorylated variant of histone H2A ( $\gamma$ H2Av), an early and specific marker of DNA damage, were observed in *mx*c mutant testes (Figures 4A–4C). Indeed, the level of  $\gamma$ H2Av observed in germ cells of *mx*c<sup>G46</sup> mutant testes was similar to the level observed in wild-type flies fed the replicative stress-inducing agent hydroxyurea (HU) (Figures 4B and 4C). In addition, high levels of  $\gamma$ H2Av were observed in CySC clones homozygous mutant for *mx*c<sup>G48</sup> (Figures 4E–4E'), suggesting that activation of the DDR correlates with loss of *mx*c.

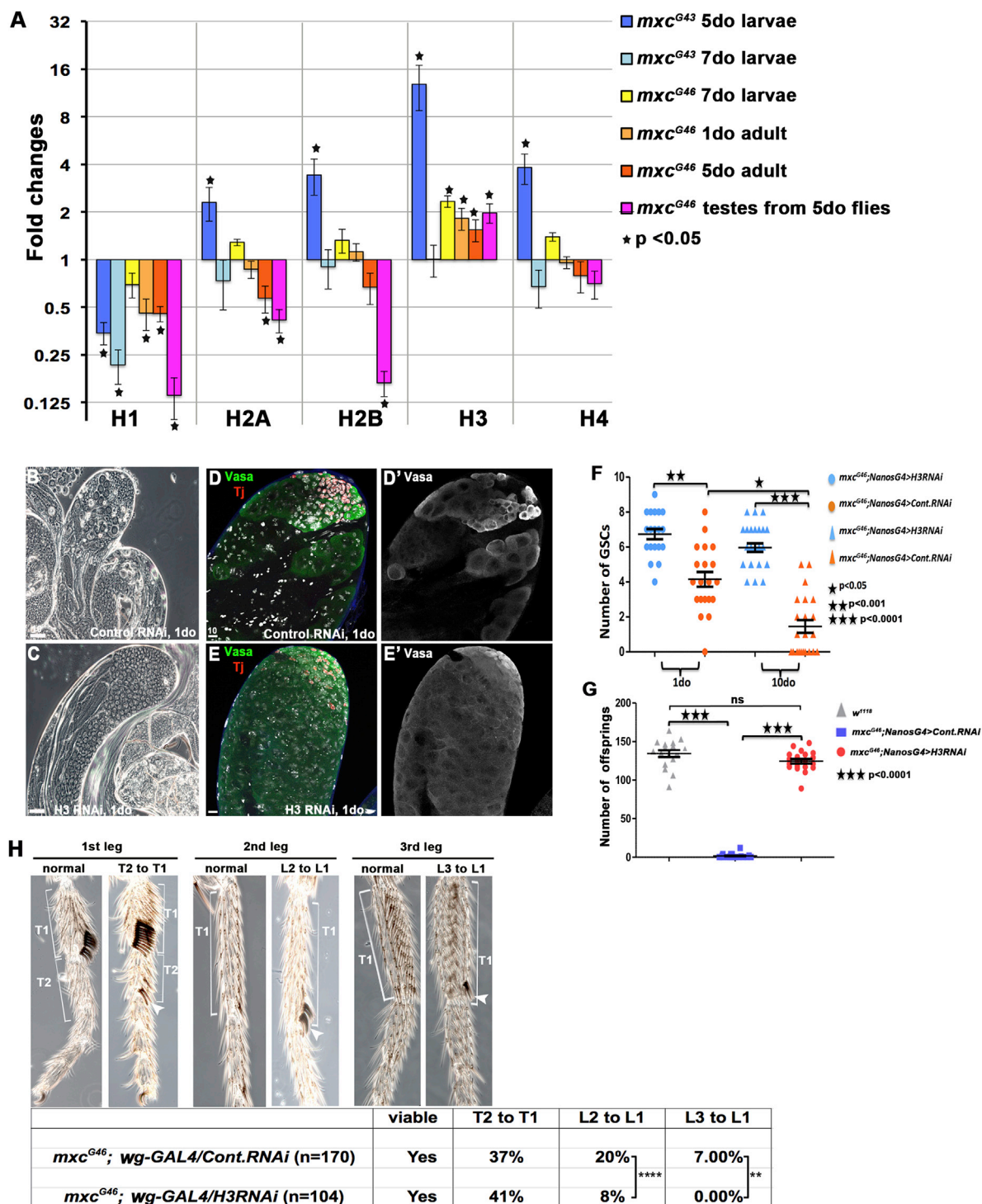
The DDR appears to be due to the increase in H3, because a decrease in the intensity of  $\gamma$ H2Av staining is observed in *mx*c<sup>G46</sup> mutant germ cells expressing H3 RNAi (Figures 4A, 4C, and 4D). In addition, GSCs in testes from *mx*c<sup>G46</sup> males expressing H3 RNAi show fewer  $\gamma$ H2Av foci and less intense staining than in *mx*c<sup>G46</sup> mutant GSCs (Figures 4F and 4H). In summary, our data suggest that changes in the normal histone mRNA levels, due to *mx*c mutations, induce replicative stress, which can be suppressed by a reduction in histone H3.

Consistent with this model, hallmarks of the *mx*c mutant germ cell phenotype were observed when we induced replicative stress and DNA damage by continuously feeding wild-type flies with HU. In 86% of the testes examined (n = 58), loss of early germ cells and the presence of cysts containing less than 16 spermatocytes were observed at the apical tip of the testis (Figures 4I and 4J). This implies that loss of stem cells and precocious differentiation observed in *mx*c<sup>G46</sup> mutants could be due solely to the replicative stress induced by persistently high H3 levels.

### **Reduced Efficiency of the DNA Damage Response Enhances *mx*c Germline Phenotypes**

At early time points, *mx*c<sup>G46</sup> mutant germ cells exhibit premature initiation of differentiation, at the expense of continued proliferation (TA divisions) (Figures 1E–1G). However, at later time points, cells appear to stall or accumulate in S phase (Figures 1G, 1I, and 1O) and exhibit hallmarks of a DDR (Figures 4C, 4E, and 4F), suggesting that cells may exhibit a protracted S phase to attempt DNA repair. Therefore, we hypothesized that abrogating a DDR should enhance the *mx*c<sup>G46</sup> testis phenotype, which would be represented by an accelerated loss of early germ cells.

Indeed, inhibition of a DDR by mutations in the H2A variant, H2Av, enhanced the *mx*c testis phenotype. H2Av serves as the functional ortholog of both H2Az and H2Ax in mammalian systems (Clarkson et al., 1999; Madigan et al., 2002).





Phosphorylation at Ser137 within the C terminus of *Drosophila* H2Av is one the earliest events in the DDR and is required to enhance DDR efficiency (Madigan et al., 2002). Null mutations in H2Av, such as *H2Av*<sup>810</sup>, are lethal but viability is rescued by either a wild-type transgene or C-terminal deleted version of H2Av (*H2Av*<sup>ΔCT</sup>) lacking the last 14 amino acids, including Ser137 (Clarkson et al., 1999; Madigan et al., 2002).

Consistent with our prediction, testes from *mx<sup>c</sup>*<sup>G46</sup>, *H2Av*<sup>ΔCT</sup>, *H2Av*<sup>810</sup>/*TM6b* males display an acceleration of the *mx<sup>c</sup>*<sup>G46</sup> phenotype, which is now evident in larval (L3) gonads (Figures 5A–5C and 5G). In addition, more than 63% (n = 82) of testes from 1 d.o. *mx<sup>c</sup>*<sup>G46</sup>, *H2Av*<sup>ΔCT</sup>; *H2Av*<sup>810</sup>/*TM6b* flies exhibit an accumulation of EdU<sup>+</sup> cells (Figures 5F and 5F'). Therefore, impairing the efficiency of the DDR extends the time required for *mx<sup>c</sup>* mutant germ cells to resolve the effects of replicative stress and accelerates the onset of germline phenotypes (cf. Figures 1F–1H and Figures 5A–5G).

### Reduced Efficiency of the DNA Damage Response Enhances Polycomb Phenotypes

In addition to enhancing the *mx<sup>c</sup>* germline phenotype, abrogation of a DDR by mutations in *H2Av* also enhances the presence of ectopic sex combs in *mx<sup>c</sup>* mutants. Loss of one copy of *H2Av* significantly enhanced the frequency of L2 to L1 and L3 to L1 transformations in *mx<sup>c</sup>*<sup>G46</sup> males (Figure 5H). In the presence of the *H2Av*<sup>ΔCT</sup> transgene, which rescues viability of *H2Av*<sup>810</sup> mutant males but cannot be phosphorylated in response to DNA damage, the frequency of L2 to L1 and L3 to L1 transformations was also significantly higher than in the *mx<sup>c</sup>* mutant background (Figure 5H). Therefore, altering a DDR by blocking phosphorylation of H2Av appears to enhance homeotic transformations typically observed as a consequence of loss of PcG function.

## DISCUSSION

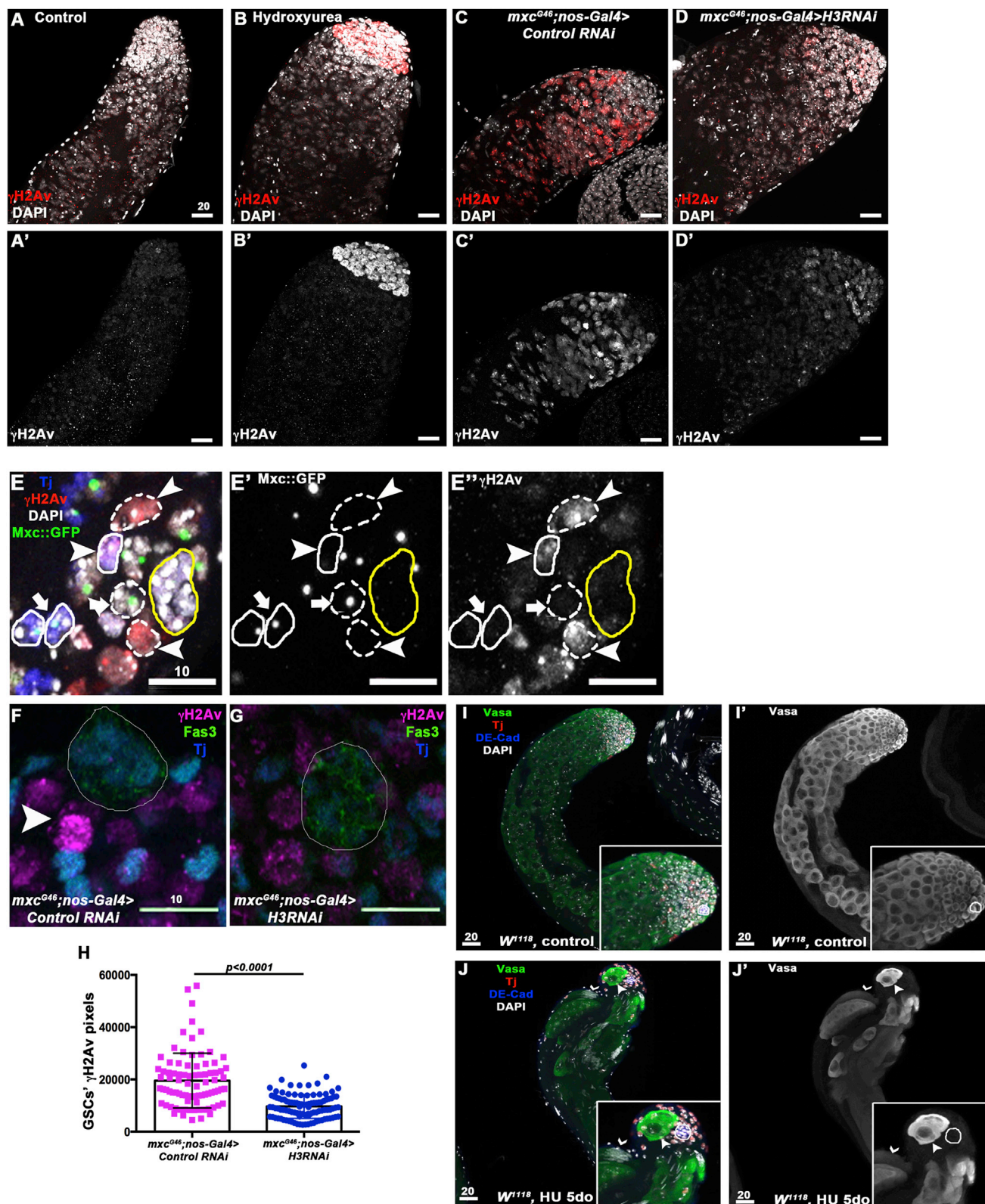
Our findings reveal that sustained levels of replicative stress and an ongoing DNA damage response can interfere with maintenance of cell-fate decisions and tissue homeostasis. Defects in histone synthesis, resulting in higher histone levels, constitute a pernicious intracellular source of replicative stress: it persists while the cells attempt to repair DNA and will reoccur cyclically in subsequent S phases. Accordingly, an intense DDR is observed both in *mx<sup>c</sup>* mutant germline and somatic cells (Figure 4). Importantly, induction of replicative stress via another mechanism, i.e., continual exposure to hydroxyurea, recapitulated the *mx<sup>c</sup>* germline phenotypes, including loss of germ cells due to premature initiation of differentiation (Figures 4I and 4J). Therefore, we suggest that a widespread and persistent DDR contributes to the precocious initiation of differentiation in *mx<sup>c</sup>* mutant cells. Due to the degree of EdU incorporation in germ cells within *mx<sup>c</sup>* mutant testes, we conclude that germ cells undergo a protracted S phase followed, ultimately, by germ

cell loss. However, given the apparent DNA damage in *mx<sup>c</sup>* mutant cells, it is possible that germ cells are in G2 but continue to incorporate EdU as a consequence of DNA repair. Nonetheless, entry into mitosis is noticeably lacking in *mx<sup>c</sup>* mutant germ cells, as indicated by an absence of phosphorylated histone H3 (Figures S1, S1F and S1F').

One outstanding question is whether the *mx<sup>c</sup>* germline and hematopoietic defects described here and elsewhere truly reflect a loss of Polycomb function. Although a role for PcG in regulating stem cell behavior and maintenance of cell identity is well established (Sauvageau and Sauvageau, 2010), a bona fide PcG phenotype in the *Drosophila* male germline has not been described previously. Elegant experiments by Chen et al. demonstrated that several PRC1 components are recruited to the nucleolus in spermatocytes upon terminal differentiation, suggesting that PcG activity may be required in early germ cells to repress the expression of differentiation genes (Chen et al., 2005). Interestingly, loss of the *Drosophila* PRC1 members *Psc* [Mel18] and *Su(z)2* [Bmi1] in germ cells did not result in loss of GSCs (Morillo Prado et al., 2012), which may suggest a different PRC1 composition in male germ cells. Moreover, the mammalian homolog of Mxc, NPAT, plays a role in DNA repair by regulating the expression of ATM (Ataxia telangiectasia mutated), in addition to H2 and H4 (Medina et al., 2007; White et al., 2011). Therefore, it is possible that *mx<sup>c</sup>* plays additional roles in mediating a DNA damage response, which would render *mx<sup>c</sup>* mutant cells more sensitive to replicative stress.

Although mutations in histones have previously been shown to reproduce or enhance Polycomb phenotypes (Lewis et al., 2013; Pengelly et al., 2013; Swaminathan et al., 2005), we report here a sustained/hindered DDR enhancing a classical PcG phenotype in vivo (Figure 5H). However, it remains unclear how replicative stress and a persistent DDR could influence Polycomb activity, leading to homeotic transformations such as those observed in *mx<sup>c</sup>* mutants. Recent evidence has implicated PcG proteins in DDR pathways; however, the precise role for PcG proteins in DNA repair has not yet been elucidated. One possibility is that PcG-mediated modification of histones is required for the change in chromatin conformation necessary to allow access of DNA repair machinery to the DNA (Chagraoui et al., 2011; Huertas et al., 2009; Vissers et al., 2012). Alternatively, PcG activity could serve to repress transcription while repair is ongoing (Chagraoui et al., 2011). Both histone H2A and H2Av are mono- and polyubiquitinated during a DDR, including monoubiquitination by PRC1 at Lys118 (Vissers et al., 2012). Therefore, an incessant induction of a DDR, such as in the case of *mx<sup>c</sup>* mutation, could result in persistent, high levels of ubiquitination at sites of DNA repair, which may interfere with the normal dynamic of monoubiquitination/deubiquitination of H2Av on Lys118 necessary for PcG-mediated repression (Scheuermann et al., 2010). On the other hand, a persistent DDR could alter PcG activity by recruiting PcG proteins to sites of DNA damage and away from normal target genes that regulate

(H) In wild-type males, sex combs are positioned on the first tarsus (T1) of the first leg (L1), but ectopic sex combs appear on T2 of L1, T1 of L2, and T1 of L3 of *mx<sup>c</sup>*<sup>G46</sup> males, resulting in partial transformations of T2 to T1, L2 to L1, and L3 to L1, respectively. Conditional expression of H3 RNAi during development reduces the L2 to L1 and L3 to L1 transformations (Table). Error bars represent SD.



(legend on next page)



cellular identity and cell-fate decisions. Regardless of whether PcG proteins play an active role in DNA repair, our data provide evidence *in vivo* that Polycomb activity can be influenced by persistent DNA damage. Therefore, we propose that any moderate, continuous source of replicative stress during development and/or in adult stem cell lineages could trigger aberrant gene expression and alterations in cell-fate decisions.

## EXPERIMENTAL PROCEDURES

### *Drosophila* Stocks and Husbandry

Flies were raised at 25°C on standard cornmeal-molasses agar medium. All *mxc* alleles ( $w^1 mxc^{G43}/FM7c$ ,  $y^1 ac^1 mxc^{G48}/FM7a$ , and  $w^1 mxc^{G46}/FM7a$ ), stocks for clonal analysis ( $Tt^1 P(neoFRT)40A/CyO$ ), RNAi-mediated depletion ( $H3$  RNAi:  $y[1] sc[*] v[1]$ ;  $P[y[+t7.7] v[+t1.8]] = TriP.GL00255)attP2$ ,  $H1$  RNAi:  $y^1 sc^* v^1$ ;  $P[TriP.GL00081)attP2$ ,  $GAL4$  RNAi:  $y[1] sc[*] v[1]$ ;  $P[y[+t7.7] v[+t1.8]] = VALIUM20-GAL4.1)attP2$ ), stock carrying  $P(tubP-GAL80[ts]7, P(tub-GAL4)1$  and the  $w^+$ ;  $P(GAL4-wg.M)MA1$  stock were obtained from the Bloomington stock center. Experiments involving  $mxc^{G46}$  adults were performed on testes from  $mxc^{G46}$  male progeny from  $mxc^{G46}/FM7a$  females outcrossed to  $w^{1118}$  males. Male  $mxc^{G43}$  or  $mxc^{G46}$  mutant larvae were selected from  $mxc^{G43}/FM7c$ ,  $Kr-GAL4$ ,  $UAS-GFP$ , or  $mxc^{G46}/FM7c$ ,  $Kr-GAL4$ ,  $UAS-GFP$  stocks based on the absence of GFP expression (Casso et al., 2000). The  $c587GAL4$  driver line was a gift from Ting Xie, and the  $nanosGAL4:VP16$ ,  $UAS-GFP$  driver was initially described in Van Doren et al., (1998).

Stocks carrying  $Sa::GFP$  (Chen et al., 2005) and  $Myc::Can$  (Hiller et al., 2001) tagged proteins were generously provided by Xin Chen and Margaret Fuller, respectively. The  $mxc^{G48}$ ,  $Sa::GFP$  line was generated by recombining the  $Sa::GFP$  transgene and  $mxc^{G48}$  allele onto the same X chromosome. Control flies, when not otherwise specified, were from an isogenized  $w^{1118}$  stock provided by D. Walker.

Stocks carrying the X-linked  $H2Av^{\Delta CT}$  transgene was generated by Clarkson et al. (1999), and flies were kindly provided by Yikang Rong. The stock  $H2Av^{\Delta CT};H2av^{810}/TM6Ubx$  was generated using the Bloomington stock  $w^+$ ;  $His2Av^{810}/TM3,Sb^1$ . Flies of the genotype  $H2Av^{\Delta CT};H2av^{810}/H2av^{810}$  were frequently observed, validating that the  $H2Av$  rescues viability of the  $H2av^{810}/H2av^{810}$  mutants. The  $H2Av^{\Delta CT}$  transgene was recombined with the  $mxc^{G46}$  allele onto the same X chromosome to generate  $mxc^{G46};H2Av^{\Delta CT}$  flies. In contrast to  $H2Av^{\Delta CT};H2av^{810}/H2av^{810}$  flies,  $mxc^{G46};H2Av^{\Delta CT};H2av^{810}/H2av^{810}$  flies are not viable. Therefore, experiments were conducted using  $mxc^{G46};H2Av^{\Delta CT};H2av^{810}/TM6b$  flies.

A stock carrying the heat-shock inducible  $H3.3::GFP$  was generously provided by Kami Ahmad (Ahmad and Henikoff, 2002).

### Generation of *mxc::GFP* Transgenic Flies

The *mxc::GFP* transgene was generated as follows: the entire *mxc* (CG12124) coding region (including introns) in addition to 625 bp upstream of the *mxc* start codon (promoter region between *mxc* and *dLarp7/CG42569*) were PCR amplified and cloned in frame with GFP into the  $\phi$ C31-based transformation

vector pattB (a gift from Johannes Bischof, Basler lab, Zurich). The GFP open reading frame was inserted between the last *mxc* codon before the stop codon (TGA) and the *mxc* 3' UTR. DNA was sent for injection to Genetic Services. The  $\phi$ C31 system was used with the *attP40* landing site on the second chromosome. Three lines were obtained, and all three exhibited the same GFP staining pattern for *Mxc::GFP*.

### Fertility Test

Single 1–2 d.o. male progeny from  $w^{1118}$  stocks (control) or  $mxc^{G46};nanosG4 > Gal4RNAi$  or  $mxc^{G46};nanosG4 > H3RNAi$  crosses were mated to three  $w^{1118}$  virgin females (30 males total for each genotype) at 25°C. Parents were removed from the vials 4 days later, and adult progeny were counted 10 days after the crosses were established. The experiment was performed in duplicate: males used initially were crossed again 5 days later to new virgin females. Statistical significance of the results was determined using GraphPad Prism, and after evaluation of the normality of the values, the Kruskal-Wallis test was applied. Both experiments (with 1–2 d.o. males or 5 d.o. males) gave the same result.

### Clonal Analysis

For clonal analysis, the *mxc::GFP* transgene was recombined onto the *FRT40A* chromosome (carrying a neomycin resistance gene), and a  $mxc^{48}/FM7$ ; *mxc::GFP-FRT40A/CyO* stock was generated. Those females were crossed to *FRT40A/CyO*; *hsFLP/MKRS* males, and viable  $mxc^{48}/Y$ ; *mxc::GFP-FRT40A/FRT40A*; *hsFLP/+* males were recovered. Those males were heat shocked twice a day (morning and evening) for 2 days during 30 min at 37°C in a circulating water bath and maintained at room temperature (22°C–23°C) between heat shocks. Clone induction was visualized by loss of the *Mxc::GFP* nuclear body in *Vasa*<sup>+</sup> germ cells (GSCs) or *Tj*<sup>+</sup> cells adjacent to the hub (CySCs). To address GSC maintenance, testes were dissected after 3 or 10 days post heat shock. The number of testes with at least one GFP<sup>+</sup> GSC was used as a readout of clone induction and GSC maintenance.

### RNAi-Mediated Knockdown of Gene Expression

Specific depletion of *mxc* from cyst cells was obtained using an *mxc* RNAi line from the Harvard TriP stock collection ( $mxc^{JF01992}$ , BL25970) expressed under the control of the cyst cell driver *c587GAL4* in combination with *GAL80<sup>ts</sup>* to repress *GAL4* activity. The *GAL4* RNAi TriP line (BL35784) was used as a negative control. The flies were maintained at 18°C–20°C until pupariation and were shifted to 29°C to activate RNAi expression until eclosion. Similar results were obtained using an independent *mxc* RNAi line from VDRC (v42978) expressed with *c587GAL4*. For these experiments, flies were raised and maintained at 25°C.

Reduction of *H3* and *H1* in the germline of  $mxc^{G46}$  males was achieved using the *H3* RNAi TriP lines expressed under the control of the *nanosGAL4:VP16*, *UAS-GFP* driver (Van Doren et al., 1998), and the *GAL4* RNAi line (BL35784) was used as a negative control. Conditional expression of *H3* RNAi to target sex combs specification during development was achieved by crossing  $mxc^{G46}$ ; *Wingless-GAL4/TM6Ubx* females to *GAL80<sup>ts</sup>/CYO;H3RNAi* or *GAL4RNAi* males.

## Figure 4. Persistent Replicative Stress Leads to Premature Differentiation and Germline Loss

(A–B') Little to no staining for  $\gamma$ H2Av is observed in control testes (A and A'). Hydroxyurea treatment induces replicative stress in mitotic germ cells leading to accumulation of  $\gamma$ H2Av (red) at the testis tip (B and B'). (C–D') Intense staining for  $\gamma$ H2Av is observed in testes from  $mxc^{G46}$  males (C and C'), which is reduced upon *H3* RNAi expression in early germ cells (D and D'). (E–E') Clone induction in the testis using the null mutant allele of *mxc*,  $mxc^{G48}$ . The *Tj*<sup>+</sup> cell (blue) adjacent to the hub (yellow circle) circled by a solid line and indicated by an arrowhead represents a CySC mutant for *mxc* (as shown by the loss of *Mxc::GFP*, E') with high level of  $\gamma$ H2Av in comparison to wild-type cyst cells (solid circle, arrow, E'). As expected,  $mxc^{G48}$  mutant germ cell clones (dashed line, arrowhead) also express high level of  $\gamma$ H2Av compared to wild-type germ cells (dashed line, arrow). (F–H) *mxc* mutant GSCs display saturation of  $\gamma$ H2Av staining (magenta, (F), arrowhead), which is less frequent and intense upon RNAi-mediated reduction in *H3*. (G) Cyst cells (*Tj*<sup>+</sup>, blue); hub (Fas3<sup>+</sup>, green). The levels of  $\gamma$ H2Av are significantly reduced in GSCs expressing *H3* RNAi (H). (I–J') Prolonged exposure to hydroxyurea recapitulates *mxc* phenotypes. (I–I') Testes from control flies contain early germ cells at the tip (hub is circled, DE-Cad<sup>+</sup>, blue), followed by growing spermatocytes. Germ cells (*Vasa*<sup>+</sup>, green); early cyst cells (*Tj*<sup>+</sup>, red). (J and J') Wild-type flies fed hydroxyurea for 5 consecutive days are depleted for early germ cells and contain cysts with fewer than 16 cells (arrowhead) close to the hub (circled), indicating incomplete TA divisions and precocious differentiation. Germ cells undergoing terminal differentiation are also present at the tip of the testes, as shown by cysts of elongating spermatids (thin arrowhead). Scale bars are in  $\mu$ m. Error bars represent SD.

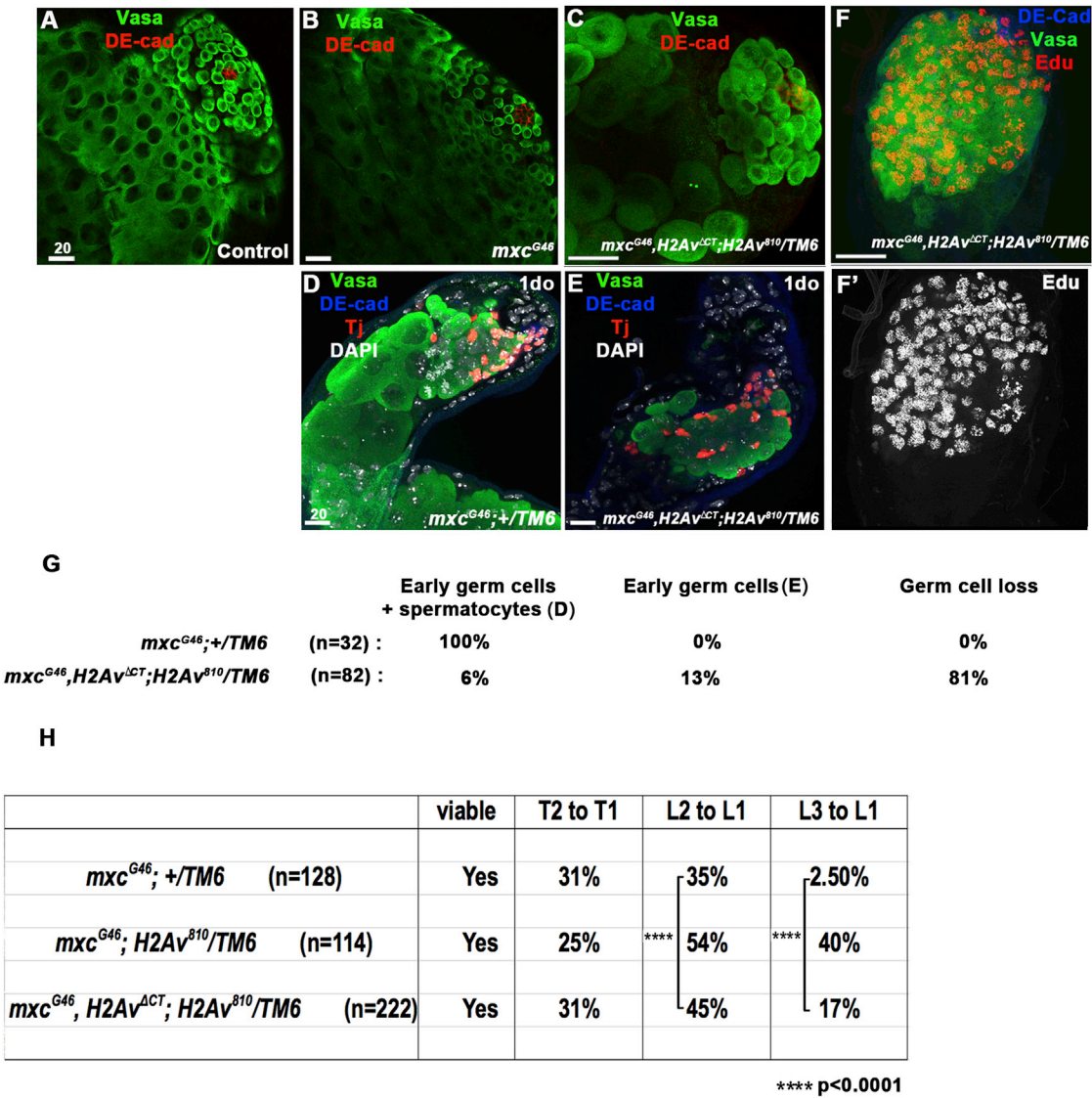


**Figure 5. Mutations in *H2Av* Enhance the Onset of *mx<sup>c</sup>* Germline Phenotypes and Ectopic Sex Combs**

(A–D) Male gonads from (A) wild-type and (B) *mx<sup>c</sup><sup>G46</sup>* third instar larvae appear wild-type, whereas the *mx<sup>c</sup>* mutant phenotype is detected at this stage in *mx<sup>c</sup><sup>G46</sup>, H2Av<sup>ΔCT</sup>; H2Av<sup>810</sup>/TM6b* (C) male larvae. Germ cells (Vasa<sup>+</sup>, green); hub (DE-cad<sup>+</sup>, red). (D and G) Testes from 1-day old *mx<sup>c</sup><sup>G46</sup>* adults, exhibit a combination of early germ cells and large germ cells that have initiated differentiation prematurely. Germ cells (Vasa<sup>+</sup>, green); hub (DE-cad<sup>+</sup>, blue); cyst cells (Tj<sup>+</sup>, red). (E–G) Testes from 1-day old *mx<sup>c</sup><sup>G46</sup>, H2Av<sup>ΔCT</sup>; H2Av<sup>810</sup>/TM6b* flies accumulate spermatogonia that appear to be stalled in S phase, as indicated by Edu incorporation. (H) The L2 to L1 and L3 to L1 transformations are enhanced in *mx<sup>c</sup><sup>G46</sup>, H2Av<sup>810</sup>/TM6b* and *mx<sup>c</sup><sup>G46</sup>, H2Av<sup>ΔCT</sup>; H2Av<sup>810</sup>/TM6b* flies.

**EdU Incorporation Experiments**

EdU incorporation was done using the Click-iT EdU Imaging kit (Invitrogen) according to manufacturer instructions. Briefly, testes were dissected in 1 × Ringer's buffer (NaCl 155 mM, KCl 5 mM, CaCl<sub>2</sub> 2 mM, MgCl<sub>2</sub> 1 mM, NaH<sub>2</sub>PO<sub>4</sub> 2 mM, HEPES 10 mM, glucose 10 mM) and incubated in a 30 μM EdU/1 × Ringer's buffer solution during 30 min. Testes were fixed 20 min in 4% formaldehyde, washed twice 5 min in 3% BSA/1 × PBS, and incubated 20 min in 1 × PBS-0.5% Triton X-100 (PBST). Testes were next incubated 30 min with the Click-iT reaction cocktail, rinse and subsequently blocked in 3% BSA/PBST. Samples were then subjected to the regular IF protocol.

**Hydroxyurea Treatment**

For acute treatment with hydroxyurea (HU), flies were starved for 8 hr before being exposed overnight to a regular vial of fly food containing a Kimwipe soaked in a grape juice 10 mg/ml HU solution. Testes were dissected 16 hr later. For the prolonged exposure to HU, flies were maintained at 25°C for 5 days in a vial of fly food mixed with 3 mg/ml HU.

**Immunofluorescence and Microscopy**

Immunofluorescence (IF) was performed on whole-mount testes dissected in PBS and fixed in 2% paraformaldehyde as previously described (Boyle et al., 2007).

Antibodies used were as follows: rabbit anti-Vasa (1:5,000, a gift from P. Lasko); mouse anti-Fas3 (7G10) (1:20), rat anti-DECadherin (DCAD2)(1:20), mouse anti-Myc 9E10 (1:50) obtained from the Developmental Studies Hybridoma Bank developed under the auspices of the National Institute of Child Health and Human Development and maintained by the University of Iowa; guinea pig anti-traffic jam (Tj) (1:3,000, a gift from D. Godt), rabbit anti-FLASH (1:1,000) and rabbit anti-Mxc (1:1,000) (gift from W. Marzluff), rabbit anti-GFP (1:5,000, Invitrogen); and rabbit H2AvD pS137 antibody (anti- $\gamma$ H2Av, 1:1,000, Rockland), mouse anti-pHH3 (1:400, Cell Signaling Technology), and rabbit anti-H1 (*Drosophila* specific, 1:1,000, Active Motif). Tissues were mounted in Vectashield with DAPI (Vector Laboratories). Secondary antibodies were obtained from Invitrogen and used 1:400.

Mounting of legs to quantify sex combs was performed as follows: fly legs were dissected in 1 × PBS and boiled 10 min in 10% KOH. Samples were washed twice with water and twice with 100% ethanol. A mix of lactic acid/ethanol (6/5) was added, and the legs were mounted on slides.

Phase contrast images of squashed testes and fly legs were obtained using a Leica DM5000 microscope equipped with a DC500 camera using Firecam imaging software (version 1.7.1; Leica Microsystems). All other images were obtained using a Zeiss LSM 710/780 Laser Scanning confocal microscope. All experiments involving cell counts and pixel quantification were performed using multiple sections (Z-stacks) from confocal images. Image processing, area measurement, and pixel quantification were executed with ImageJ 1.45r (Wayne Rasband, National Institute of Health, <http://imagej.nih.gov/ij>).

## FISH

FISH was performed as described in [Toledano et al. \(2012\)](#). The entire open reading frame of the histone H3 gene was used as a probe.

## Quantitative Real-Time PCR

RNA was extracted using TRIzol (Invitrogen) according to manufacturer's instructions. After DNase treatment (RQ1, Promega), RNA was quantified and 300 ng were used in each reverse transcription reaction (Superscript III First Strand, Invitrogen). For the PCR, 1/12 of cDNA, 0.2  $\mu$ M primers, and 1 × SYBR Green mix (Applied Biosystems) were used with the following cycle in a ABI Prism cycler: 10 min 95°C, (15 s 95°C, 45 s 60°C) 39×. The primers used were as follows: H1-f (5'-GCA AAA GCC AAG GAT GCC AAG AAA ACT G-3'), H1-r (5'-ACT TTT TGG CAG CCG TAG TCT TCG-3'), H2A-f (5'-GCT GGC AAT GCT GCT CGT GAC AA-3'), H2A-r (5'-AGG CCT TCT TCT CGG TCT TCT TG-3'), H2B-f (5'-GAA GGC GAT GAG CAT AAT GAA CAG CT-3'), H2B-r (5'-ATT TAG AGC TGG TGT ACT TGG TGA C-3'), H3-f (5'-AGA CGG ACT TGC GAT TCC AGA GC T-3'), H3-r (5'-AAG CAC GCT CGC CGC GAA TG-3'), H4-f (5'-GCG GTG TGA AGC GCA TAT CTG GA-3'), H4-r (5'-AAC CGC CAA ATC CGT AGA GGG T-3'), GAPDH-f (5'-GCG GTA GAA TGG GGT GAG AC-3'), and GAPDH-r (5'-TGA AGA GCG AAA ACA GTA GC-3'). Each sample was duplicated on the PCR plate, and the final results average three biological replicates. For the quantification, the comparative  $C_T$  method was used after the primers efficiency was verified and validated in a plot of log input amount versus  $\Delta C_T$ .

## Statistical Analysis

All quantitative experiments were evaluated for statistic significance using the software GraphPad prism, after verifying the normality of values and equivalence of variances. For the quantitative RT-PCR, each sample was duplicated on the PCR plate, and the final results average the  $\Delta\Delta C_T$  of three biological replicates. The statistical significance of observed differences in the fold changes was tested against a theoretical mean equal to 1 in a one sample Student's t test. For stem cell counts and pixel quantification, the statistical differences between mutant or RNAi-treated samples and controls were addressed using a Student's two-tailed t test. For the sex combs phenotype on male legs, results were translated into individual contingency tables for each legs, where each row defines a genetic background (for example,  $mxc^{G46}, H2Av^{WT}$  versus  $mxc^{G46}, H2Av^{\Delta CT}$ ), each column defines an outcome (normal leg or leg with misplaced sex combs) and each value is an exact count. Statistical significance was assayed using a two-sided chi-square test. Statistical significance was concluded whenever the calculated  $p < 0.05$ .

## SUPPLEMENTAL INFORMATION

Supplemental Information includes three figures and can be found with this article online at <http://dx.doi.org/10.1016/j.celrep.2014.03.042>.

## ACKNOWLEDGMENTS

We are grateful to P. Lasko, D. Godt, and R. Glaser for generous gifts of antibodies; M. Fuller, X. Chen, Y. Rong, and K. Ahmad for sharing fly stocks; N. Randsholt for information regarding *mxc* alleles; R. Duronio and W. Marzluff for sharing reagents, fly stocks, and data prior to publication; and Jonah Cool, Kathrin Plath, and members of the Jones lab who contributed to constructive discussions. We thank the TRiP at Harvard Medical School (NIH/NIGMS R01-GM084947) for providing transgenic RNAi fly stocks used in this study and the Bloomington stock center. This work was supported by a Pioneer Award from the Salk Institute (to S.L.), the G. Harold and Leila Y. Mathers Charitable Foundation, the American Federation for Aging Research, the California Institute for Regenerative Medicine, and the NIH (to D.L.J.).

Received: May 30, 2013

Revised: January 16, 2014

Accepted: March 13, 2014

Published: April 17, 2014

## REFERENCES

- Ahmad, K., and Henikoff, S. (2002). The histone variant H3.3 marks active chromatin by replication-independent nucleosome assembly. *Mol. Cell* 9, 1191–1200.
- Becker, K.A., Ghule, P.N., Lian, J.B., Stein, J.L., van Wijnen, A.J., and Stein, G.S. (2010). Cyclin D2 and the CDK substrate p220(NPAT) are required for self-renewal of human embryonic stem cells. *J. Cell. Physiol.* 222, 456–464.
- Boyle, M., Wong, C., Rocha, M., and Jones, D.L. (2007). Decline in self-renewal factors contributes to aging of the stem cell niche in the *Drosophila* testis. *Cell Stem Cell* 1, 470–478.
- Brand, A.H., Manoukian, A.S., and Perrimon, N. (1994). Ectopic expression in *Drosophila*. *Methods Cell Biol.* 44, 635–654.
- Casso, D., Ramirez-Weber, F., and Kornberg, T.B. (2000). GFP-tagged balancer chromosomes for *Drosophila melanogaster*. *Mech. Dev.* 91, 451–454.
- Chagraoui, J., Hébert, J., Girard, S., and Sauvageau, G. (2011). An anticlastogenic function for the Polycomb Group gene Bmi1. *Proc. Natl. Acad. Sci. USA* 108, 5284–5289.
- Chen, X., Hiller, M., Sancak, Y., and Fuller, M.T. (2005). Tissue-specific TAFs counteract Polycomb to turn on terminal differentiation. *Science* 310, 869–872.
- Clarkson, M.J., Wells, J.R., Gibson, F., Saint, R., and Tremethick, D.J. (1999). Regions of variant histone His2AvD required for *Drosophila* development. *Nature* 399, 694–697.
- Docquier, F., Saget, O., Forquignon, F., Randsholt, N.B., and Santamaria, P. (1996). The multi sex combs gene of *Drosophila melanogaster* is required for proliferation of the germline. *Dev. Genes Evol.* 205, 203–214.
- Fuller, M. (1993). Spermatogenesis. In *The Development of Drosophila*, M. Bate and A. Martinez-Arias, eds. (Cold Spring Harbor: Cold Spring Harbor Laboratory Press).
- Ghule, P.N., Dominski, Z., Yang, X.-C., Marzluff, W.F., Becker, K.A., Harper, J.W., Lian, J.B., Stein, J.L., van Wijnen, A.J., and Stein, G.S. (2008). Staged assembly of histone gene expression machinery at subnuclear foci in the abbreviated cell cycle of human embryonic stem cells. *Proc. Natl. Acad. Sci. USA* 105, 16964–16969.
- Gonczy, P., and DiNardo, P.G.S. (1996). The germ line regulates somatic cyst cell proliferation and fate during *Drosophilaspermato*genesis. *Development* 122, 1–12.



- Gunjan, A., and Verreault, A. (2003). A Rad53 kinase-dependent surveillance mechanism that regulates histone protein levels in *S. cerevisiae*. *Cell* 115, 537–549.
- Herrero, A.B., and Moreno, S. (2011). Lsm1 promotes genomic stability by controlling histone mRNA decay. *EMBO J.* 30, 2008–2018.
- Hiller, M.A., Lin, T.Y., Wood, C., and Fuller, M.T. (2001). Developmental regulation of transcription by a tissue-specific TAF homolog. *Genes Dev.* 15, 1021–1030.
- Huertas, D., Sendra, R., and Muñoz, P. (2009). Chromatin dynamics coupled to DNA repair. *Epigenetics* 4, 31–42.
- Kiger, A.A., White-Cooper, H., and Fuller, M.T. (2000). Somatic support cells restrict germline stem cell self-renewal and promote differentiation. *Nature* 407, 750–754.
- Kiger, A.A., Jones, D.L., Schulz, C., Rogers, M.B., and Fuller, M.T. (2001). Stem cell self-renewal specified by JAK-STAT activation in response to a support cell cue. *Science* 294, 2542–2545.
- Leatherman, J.L., and Dinardo, S. (2008). Zfh-1 controls somatic stem cell self-renewal in the *Drosophila* testis and nonautonomously influences germline stem cell self-renewal. *Cell Stem Cell* 3, 44–54.
- Leatherman, J.L., and Dinardo, S. (2010). Germline self-renewal requires cyst stem cells and stat regulates niche adhesion in *Drosophila* testes. *Nat. Cell Biol.* 12, 806–811.
- Lewis, E.B. (1978). A gene complex controlling segmentation in *Drosophila*. *Nature* 276, 565–570.
- Lewis, P.W., Müller, M.M., Koletsky, M.S., Cordero, F., Lin, S., Banaszynski, L.A., Garcia, B.A., Muir, T.W., Becher, O.J., and Allis, C.D. (2013). Inhibition of PRC2 activity by a gain-of-function H3 mutation found in pediatric glioblastoma. *Science* 340, 857–861.
- Madigan, J.P., Chotkowski, H.L., and Glaser, R.L. (2002). DNA double-strand break-induced phosphorylation of *Drosophila* histone variant H2Av helps prevent radiation-induced apoptosis. *Nucleic Acids Res.* 30, 3698–3705.
- Marzluff, W.F., and Duronio, R.J. (2002). Histone mRNA expression: multiple levels of cell cycle regulation and important developmental consequences. *Curr. Opin. Cell Biol.* 14, 692–699.
- Matunis, E., Tran, J., Gönczy, P., Caldwell, K., and DiNardo, S. (1997). punt and schnurri regulate a somatically derived signal that restricts proliferation of committed progenitors in the germline. *Development* 124, 4383–4391.
- Medina, R., van der Deen, M., Miele-Chamberland, A., Xie, R.-L., van Wijnen, A.J., Stein, J.L., and Stein, G.S. (2007). The HNF-P/p220NPAT cell cycle signaling pathway controls nonhistone target genes. *Cancer Res.* 67, 10334–10342.
- Morillo Prado, J.R., Chen, X., and Fuller, M.T. (2012). Polycomb group genes Psc and Su(z)2 maintain somatic stem cell identity and activity in *Drosophila*. *PLoS ONE* 7, e52892.
- Pengelly, A.R., Copur, Ö., Jäckle, H., Herzig, A., and Müller, J. (2013). A histone mutant reproduces the phenotype caused by loss of histone-modifying factor Polycomb. *Science* 339, 698–699.
- Saget, O., Forquignon, F., Santamaria, P., and Randsholt, N.B. (1998). Needs and targets for the multi sex combs gene product in *Drosophila melanogaster*. *Genetics* 149, 1823–1838.
- Salzler, H.R., Tatomer, D.C., Malek, P.Y., McDaniel, S.L., Orlando, A.N., Marzluff, W.F., and Duronio, R.J. (2013). A sequence in the *Drosophila* H3-H4 Promoter triggers histone locus body assembly and biosynthesis of replication-coupled histone mRNAs. *Dev. Cell* 24, 623–634.
- Santamaria, P., and Randsholt, N.B. (1995). Characterization of a region of the X chromosome of *Drosophila* including multi sex combs (mxc), a Polycomb group gene which also functions as a tumour suppressor. *Mol. Gen. Genet.* 246, 282–290.
- Sauvageau, M., and Sauvageau, G. (2010). Polycomb group proteins: multifaceted regulators of somatic stem cells and cancer. *Cell Stem Cell* 7, 299–313.
- Scheuermann, J.C., de Ayala Alonso, A.G., Oktaba, K., Ly-Hartig, N., McGinty, R.K., Fraterman, S., Wilm, M., Muir, T.W., and Müller, J. (2010). Histone H2A deubiquitinase activity of the Polycomb repressive complex PR-DUB. *Nature* 465, 243–247.
- Schwartz, Y.B., and Pirrotta, V. (2007). Polycomb silencing mechanisms and the management of genomic programmes. *Nat. Rev. Genet.* 8, 9–22.
- Singh, R.K., Liang, D., Gajjalaiahvari, U.R., Kabbaj, M.-H.M., Paik, J., and Gunjan, A. (2010). Excess histone levels mediate cytotoxicity via multiple mechanisms. *Cell Cycle* 9, 4236–4244.
- Sparmann, A., and van Lohuizen, M. (2006). Polycomb silencers control cell fate, development and cancer. *Nat. Rev. Cancer* 6, 846–856.
- Swaminathan, J., Baxter, E.M., and Corces, V.G. (2005). The role of histone H2Av variant replacement and histone H4 acetylation in the establishment of *Drosophila* heterochromatin. *Genes Dev.* 19, 65–76.
- Toledano, H., D’Alterio, C., Loza-Coll, M., and Jones, D.L. (2012). Dual fluorescence detection of protein and RNA in *Drosophila* tissues. *Nat. Protoc.* 7, 1808–1817.
- Tulina, N., and Matunis, E. (2001). Control of stem cell self-renewal in *Drosophila* spermatogenesis by JAK-STAT signaling. *Science* 294, 2546–2549.
- Tran, J., Brenner, T.J., and DiNardo, S. (2000). Somatic control over the germline stem cell lineage during *Drosophila* spermatogenesis. *Nature* 407, 754–757.
- Van Doren, M., Williamson, A.L., and Lehmann, R. (1998). Regulation of zygotic gene expression in *Drosophila* primordial germ cells. *Curr. Biol.* 8, 243–246.
- Vissers, J.H.A., van Lohuizen, M., and Citterio, E. (2012). The emerging role of Polycomb repressors in the response to DNA damage. *J. Cell Sci.* 125, 3939–3948.
- White, A.E., Burch, B.D., Yang, X.-C., Gasdaska, P.Y., Dominski, Z., Marzluff, W.F., and Duronio, R.J. (2011). *Drosophila* histone locus bodies form by hierarchical recruitment of components. *J. Cell Biol.* 193, 677–694.
- Xu, T., and Rubin, G.M. (1993). Analysis of genetic mosaics in developing and adult *Drosophila* tissues. *Development* 117, 1223–1237.